CONVECTIVE INSTABILITY OF A NON-UNIFORMLY VISCOUS SPHERE WITH REFERENCE TO THE EARTHS MANTLE

C. Brennen

Senior Research Fellow in Engineering Science
California Institute of Technology
Pasadena, California 91109

ABSTRACT

The principal concern of this paper is with the thermal convective instabilities of a non-uniformly viscous liquid sphere heated internally by some distribution of heat sources. Solutions are first obtained which correspond to an extension of the classic theory for uniformly viscous spheres for (1) radial variations of viscosity and (2) near critical Reynolds numbers. This results in instability growth rates which strongly suggest that the earth's mantle must have been in a highly supercritical state for the present convective pattern to have been established within the earth's lifetime. The paper then proceeds to a different theoretical calculation for incipient growth rates for such supercritical situations. For the earth's mantle this results in typical growth times of the order of 10^5 years. Various outer boundary conditions of the fixed and free type are explored; a true free surface condition is also examined and results in the establishment of a Froude number-like parameter governing distortion of the outer surface. In addition it is demonstrated that the spherical harmonics of degree 3 or 4 which seem to dominate the present convective pattern in the earth's mantle would do so in the theoretical construction if the increase of viscosity with depth within the mantle were such that the deep mantle viscosity was some four times the upper mantle value.

1. INTRODUCTION

The principal objective of this paper is to investigate the thermal convective instability of a non-uniformly viscous liquid sphere whose interior is maintained at a higher temperature than the surface due to some distribution of internal heat sources. The classical problem in which the liquid of the sphere is uniformly viscous has been examined by many authors in the past and a chapter is devoted to the subject in Chandrasekhar's (1961) book. The present work is an extension to the case in which the viscosity is a function of radial distance from the center. As discussed by Chandrasekhar (1961), Vening Meinesz (1964) and Heiskanen and Vening Meinesz (1958) one of the particularly intriguing applications of such analyses is to the stability of the earth's mantle not only for the present time but throughout its history.

Following the work of Pekeris (1935), Hales (1936), Heiskanen and Vening Meinesz (1958), Knopoff (1964) and Tozer (1965) as well as that of many eminent geologists who have studied ocean floor spreading (see Wilson (1971)) it is now fairly well established that thermal convection cell flows exist in the earths mantle. The outward spreading of the ocean floor from oceanic ridges is believed to coincide with upwelling regions and the inward motion toward deep ocean trenches, island arcs, recent mountains belts and regions of deep earthquakes appears to reflect downwelling. In many places these motions have been quantitatively assessed by paleomagnetic evidence from deep ocean cores. The pattern of motion of the surface suggested by these studies is displayed in Fig. 1 which is taken from Wilson (1971). Evidence of a different nature has been demonstrated by Runcorn (1964) who showed that

anomalies in the earth's gravitational field may be related to density variations caused by the pattern of convective flow within the mantle. Runcorn constructed the surface flow pattern which could cause these gravitational anomalies and this is reproduced in figure 2. If this represents the flow pattern at some small distance beneath the actual surface of the earth this might account for some of the discrepancies between figures 1 and 2. However both strongly indicate rolls of width between about 4000 and 8000 km. The pioneering studies of finite amplitude convection in the mantle by Turcotte and Oxburgh (1967) indicated that a cell which penetrated the complete mantle (depth 3000 km) would have a width of about 2100 km, significantly smaller than the observed widths. Though Turcotte and Oxburgh assume uniform mantle viscosity later studies by Takeuchi and Sakata (1970) have indicated an increased ratio of cell width to depth when the viscosity of the mantle increases with depth as the evidence discussed later suggests. The results of the present studies indicate a similar trend. Both figure 1 and figure 2 also suggest a velocity field which is a poloidal harmonic function of degree 3 having convection pattern "poles" in the neighborhood of 70°E., 10°N., 80°W. and 10°S. Such a mathematical surface pattern would exhibit divergent flow from the first pole, convergence toward the second pole and an "equatorial" band of flow between upwelling and downwelling regions (indicated by the dashed lines in figure 2).

The stability of uniformly viscous spheres and spherical shells is discussed at length by Chandrasekhar (1961). Briefly, for a complete sphere and for all reasonable radial variations in the body force (gravity), temperature, coefficient of thermal expansion, heat sources and thermal conductivity the most unstable flow (or that which is neutrally stable at the lowest Rayleigh number) is that which consists of a solid poloidal harmonic of the first

degree. Only when an internal boundary is inserted and the stability of the resulting spherical shell (mantle) is considered is it found that the most unstable mode becomes one of higher degree. When this boundary is placed at the estimated inner limit of the mantle so that its radius is roughly one half of that of the external boundary the most unstable mode is typically of degree 3 or 4.

But a serious criticism of the previous theoretical results is the simple fact that they assume uniform viscosity. On the other hand the viscosity of the mantle is probably not uniform. Indeed, in the not too distant past the available evidence seemed to indicate that the viscosity increase between the upper mantle and its deeper parts was as much as four orders of magnitude (e.g., McConnell (1968), Gordon (1965)). More recent theoretical studies by Weertman (1970) and re-analysis of isostatic recovery data by Brennen (1973) suggest that the increase is rather smaller, perhaps around one order of magnitude or less. It is nevertheless significant and the effect on the thermal stability of the mantle has been widely discussed. Some investigators have suggested that the viscosity variation might lead to an instability flow pattern which involved a number of cells stacked vertically rather than the single cell layer of the uniformly viscous analysis. This paper finds no evidence of such patterns of flow. In other works, Turcotte and Oxburgh (1969) have studied the effect of non-uniform mantle properties on developed convection patterns and Takeuchi and Sakata (1970) investigated the stability of a mantle model involving two layers of differing viscosities. Elsasser (1971, 1972) has further included the effect of a more solid-like crustal layer and chemical differentiation in his qualitative discussion of upper mantle convection.

Thus, one of the objectives of the present paper was to provide analyses and results which could be at least qualitatively employed to assess the effect of such viscosity variations on the thermal convective instability of the earth's mantle and to suggest the form of the consequent convective flow patterns. In order to simplify the analysis a rather simple radial variation of kinematic viscosity, $\nu(r)$, with radius r of the form

$$\nu(r) = \nu_o (r/a)^{\epsilon} \qquad (1)$$

is assumed where ν_o is the viscosity at the upper boundary of the mantle where $r = a$ and ϵ is an exponent to which various values will be assigned. The data of Brennen (1973) and the theory of Weertman (1970) suggest that ϵ for the earth's mantle may be between -3 and -10. The older studies referred to earlier would indicate values in the neighborhood of -30 (see Brennen (1973)).

2. Equations of motion for a non-uniformly viscous sphere

In this section the equations of motion for thermal convective instability in a spherical region will be constructed along conventional lines (Chandrasekhar (1961)) except that a radial variation of viscosity will be introduced. The Navier-Stokes equations of motion for a fluid of non-uniform viscosity are (Milne Thomson (1968))

$$\rho \frac{D\underline{v}}{Dt} = \rho\underline{F} - \nabla p - \mu\nabla\times(\nabla\times\underline{v}) + 2(\nabla\mu\,\nabla)\underline{v} + (\nabla\mu)\times(\nabla\times\underline{v}) \tag{2}$$

where $\underline{v}$ is the velocity vector, ρ is the density, $\underline{F}$ is the body force vector, p is the pressure, μ the dynamic viscosity and t is time. The equation of continuity is

$$\nabla\cdot(\rho\underline{v}) = 0 \quad . \tag{3}$$

The undisturbed temperature distribution, $T^*(r)$ where r, θ, φ are spherical polar coordinates, is taken to be

$$\frac{\partial T^*}{\partial r} = -2\beta(r)r \tag{4}$$

where $\beta(r)$ depends on assumptions concerning the distribution of heat sources within the sphere. This temperature is perturbed to $T^* + T(r, \theta, \varphi)$ by the onset of a motion $v(r, \theta, \varphi)$. The conventional Boussinesq approximation permits neglect of the consequent variations in density <u>except</u> in the body force (or buoyancy) term, F, of the equation of motion (2). In addition the convective inertial terms of the left hand side of that equation are negligible since they are of second order and since the resulting motions occur at Reynolds numbers very much less than unity. Thus the equations of continuity (3) and momentum (2) become

$$\nabla \cdot \underline{v} = 0 \tag{5}$$

$$\frac{\partial \underline{v}}{\partial t} = -\nabla\left(\frac{\Delta p}{\rho}\right) + \alpha g(r) T \frac{\underline{r}}{r} + \nu(r)\nabla^2 \underline{v} + \frac{\partial \nu}{\partial r}\left\{2\frac{\partial \underline{v}}{\partial r} + \frac{\underline{r}}{r} \times (\nabla \times \underline{v})\right\} \tag{6}$$

where α is the coefficient of thermal expansion, $g(r)$ is the gravitational field, $\nu(r)$ is the kinematic viscosity and Δp represents the departure of the pressure from its undisturbed value. It is convenient to denote $\alpha g(r)/r$ by $\gamma(r)$. In addition the energy or heat diffusion equation becomes

$$\frac{\partial T}{\partial t} = \kappa \nabla^2 T + 2\beta(r) r v_r \quad . \tag{7}$$

where κ is the thermal diffusivity. Taking the curl of Eq. (6) and scalar multiplying the result by $\underline{r}$ yields

$$\frac{\partial}{\partial t}(r\omega_r) = \nu\nabla^2(r\omega_r) + \frac{\partial \nu}{\partial r}\left\{\frac{\partial}{\partial r}(r\omega_r) - \omega_r\right\} \tag{8}$$

where the vorticity $\underline{\omega}$ is defined by $\nabla \times \underline{v}$. Further, taking curl^2 of Eq. (6) and scalar multiplying the result by $\underline{r}$ gives

$$\begin{aligned}\frac{\partial}{\partial t}(\nabla^2(rv_r)) = &- L^2(\gamma T) + \nu\nabla^4(rv_r) \\ &+ \frac{\partial \nu}{\partial r}\left[2\frac{\partial(\nabla^2(rv_r))}{\partial r} + \frac{2}{r}\nabla^2(rv_r) + \frac{2v_r}{r^2} - \frac{2}{r^2}\frac{\partial}{\partial r}(rv_r) - \frac{2}{r}\frac{\partial^2(rv_r)}{\partial r^2}\right] \\ &+ \frac{\partial^2 \nu}{\partial r^2}\left[-\nabla^2(rv_r) - \frac{2}{r^2}(rv_r) + \frac{2}{r}\frac{\partial(rv_r)}{\partial r} + 2\frac{\partial^2(rv_r)}{\partial r^2}\right]\end{aligned} \tag{9}$$

where the operator

$$L^2 \equiv 2r\frac{\partial}{\partial r} + r^2\frac{\partial^2}{\partial r^2} - r^2\nabla^2 \quad . \tag{10}$$

The solution to Equations (7), (8) and (9) will be sought in terms of the normal modes which involve spherical surface harmonic functions, $S_n(\theta,\varphi)$:

$$rv_r = V(r)\, S_n(\theta,\varphi)\, e^{\eta t} \tag{11}$$

$$r\omega_r = W(r)\, S_n(\theta,\varphi)\, e^{\eta t} \tag{12}$$

$$T = X(r)\, S_n(\theta,\varphi)\, e^{\eta t} \tag{13}$$

Note that a basic property of spherical harmonic functions leads to

$$\nabla^2\{F(r)\, S_n(\theta,\varphi)\} = S_n(\theta,\varphi)\, D\{F(r)\} \tag{14}$$

where

$$D \equiv \frac{\partial^2}{\partial r^2} + \frac{2}{r}\frac{\partial}{\partial r} - \frac{n(n+1)}{r^2} \tag{15}$$

and that

$$L^2\{F(r)\, S_n(\theta,\varphi)\} = S_n(\theta,\varphi)\, n(n+1)\, F(r) \tag{16}$$

Before substituting (11), (12) and (13) into the basic equations for rv_r, $r\omega_r$ and T, namely (7), (8) and (9) it is convenient to take the opportunity to non-dimensionalize the radial coordinate so that r now takes a value of unity (rather than a dimensional value) at an outer boundary. Consequently the substitution yields

$$\left[-\left(\frac{\eta a^2}{\nu_o}\right) r^{-\epsilon} + D + \frac{\epsilon}{r}\frac{\partial}{\partial r} - \frac{\epsilon}{r^2}\right] W(r) = 0 \tag{17}$$

$$\left[-\left(\frac{\eta a^2}{\nu_o}\right) r^{-\epsilon} D + D^2 + \frac{2\epsilon}{r}\frac{\partial}{\partial r} D - \frac{\epsilon(\epsilon-3)}{r^2} D - \frac{2\epsilon(\epsilon-2)}{r^4}\right.$$

$$\left. + \frac{2\epsilon(\epsilon-2)}{r^3}\frac{\partial}{\partial r} + \frac{2\epsilon(\epsilon-2)}{r^2}\frac{\partial^2}{\partial r^2}\right] V(r) = n(n+1)\frac{a^3\gamma(r)}{\nu(r)}\, X(r) \tag{18}$$

$$\left[\frac{\eta a^2}{\kappa(r)} - D\right] X(r) = \frac{2\beta(r)}{\kappa(r)} a^2 V(r) \qquad (19)$$

Further, it will be assumed that the radial variations of γ, β and κ can be represented by

$$\gamma(r) = \gamma_o r^{\sigma_\gamma} = \alpha_o g_o r^{\sigma_\gamma} \quad ; \qquad (20)$$

$$\beta(r) = \beta_o r^{\sigma_\beta} \quad ; \qquad (21)$$

$$\kappa(r) = \kappa_o r^{\sigma_\kappa} \qquad (22)$$

Then substituting $\Psi = \kappa_o X / 2\beta_o a^2$ the Equations (17), (18) and (19) become

$$\left[-\left(\frac{\eta a^2}{\nu_o}\right) r^{-\epsilon} + D + \frac{\epsilon}{r}\frac{\partial}{\partial r} - \frac{\epsilon}{r^2}\right] W(r) = 0 \qquad (23)$$

$$\left[-\left(\frac{\eta a^2}{\nu_o}\right) r^{-\epsilon} D + D^2 + \frac{2\epsilon}{r}\frac{\partial}{\partial r} D - \frac{\epsilon(\epsilon-3)D}{r^2} + \frac{2\epsilon(\epsilon-2)}{r^2}\left\{\frac{\partial^2}{\partial r^2} + \frac{1}{r}\frac{\partial}{\partial r} - \frac{1}{r^2}\right\}\right] V(r)$$

$$= n(n+1)\, R\, r^{\sigma_\gamma - \epsilon}\, \Psi(r) \qquad (24)$$

$$\left[\left(\frac{\eta a^2}{\kappa_o}\right) r^{-\sigma_\kappa} - D\right] \Psi(r) = r^{\sigma_\beta - \sigma_\kappa}\, V(r) \qquad (25)$$

where R is the surface Rayleigh Number $2\beta_o \alpha_o g_o a^5 / \kappa_o \nu_o$.

3. Boundary Conditions

Appropriate boundary conditions to be imposed at r = 1 must now be discussed. In all cases it is required that the temperature perturbation is zero at r = 1 and thus

$$T = X = \Psi = 0 \quad \text{at} \quad r = 1 \qquad (26)$$

The solution of the problem also requires two boundary conditions on the flow at r = 1. However a number of different flow boundary conditions will be considered in the present paper. In previous analyses of spherical stability

Chandrasekhar (1961) and others have imposed the condition of zero radial velocity at r = 1 which clearly requires that

$$V = 0 \quad \text{at} \quad r = 1 \tag{27}$$

This is usually accompanied by a condition of zero tangential velocities, giving a "fixed" surface at r = 1 or by a condition of zero tangential stress at the surface, which is termed a "free" surface in the literature. From the equation of continuity and the definition of vorticity it follows fairly straightforwardly that the condition of zero tangential velocity becomes

$$\left(V + r\frac{\partial V}{\partial r}\right)_{r=1} = 0 \tag{28}$$

and

$$\left(W\right)_{r=1} = 0 \tag{29}$$

Similarly it follows with some manipulation that the condition of zero tangential stress becomes

$$\left(W - r\frac{\partial W}{\partial r}\right)_{r=1} = 0 \tag{30}$$

and

$$\left(r^2\frac{\partial^2 V}{\partial r^2} + V\,(n(n+1) - 2)\right)_{r=1} = 0 \tag{31}$$

But for the sake of completeness consider a true free surface condition which requires the conditions of zero tangential stress and constant normal stress on a boundary which deviates from r = 1. This deviation may be assumed to be small since the stability of a sphere, r = 1, is being considered. Let the perturbed boundary be

$$r = 1 + \xi(\theta, \varphi, t) \quad , \quad \xi \ll r \tag{32}$$

It follows to the first order in ξ that

$$\left(v_r\right)_{r=1} = \frac{\partial \xi}{\partial t} \tag{33}$$

The condition of zero tangential stress is identical to (30), (31) to this first order. The condition of zero normal stress at the surface leads, in the first order, to

$$(\Delta p)_{r=1} = \rho_o g_o \xi + 2\mu_o \left(\frac{\partial v_r}{\partial r}\right)_{r=1} \tag{34}$$

Using the equation of motion to eliminate Δp this can be written after some manipulation as

$$-g_o L^2 \xi = \frac{\partial}{\partial t}\left\{\frac{\partial\left(r^2 v_r\right)}{\partial r}\right\} + \nu \frac{\partial}{\partial r}\left\{2L^2 v_r - r\nabla^2(r v_r)\right\}$$

$$+ r\frac{\partial \nu}{\partial r}\left\{2\frac{\partial}{\partial r}(r\omega_r) + \nabla^2(r v_r)\right\} \tag{35}$$

where all terms are evaluated at $r = 1$. Finally by differentiating this with respect to time, t, and employing (33) the normal stress condition can be written as

$$n(n+1)V = \frac{\eta \nu_o}{g_o a}\left[\begin{array}{l} -\left(\frac{\eta a^2}{\nu_o}\right)\left\{V + r\frac{\partial V}{\partial r}\right\} \\ \\ +\frac{\partial}{\partial r}\left\{rDV - \frac{2n(n+1)V}{r}\right\} - \epsilon\left\{2\frac{\partial W}{\partial r} + DV\right\} \end{array}\right] \tag{36}$$

at $r = 1$.

4. Solution of Neutrally Stable Problem

The neutrally stable solution for which $\eta = 0$ in equations [23], [24] and [25] will be considered first. The equations become

$$\left[D + \frac{\epsilon}{r}\frac{\partial}{\partial r} - \frac{\epsilon}{r^2}\right] W = 0 \qquad [37]$$

$$\left[D^2 + \frac{2\epsilon}{r}\frac{\partial}{\partial r} D - \frac{\epsilon(\epsilon-3)}{r^2} D + \frac{2\epsilon(\epsilon-2)}{r^2}\left\{\frac{\partial^2}{\partial r^2} + \frac{1}{r}\frac{\partial}{\partial r} - \frac{1}{r^2}\right\}\right] V = n(n+1) R r^{\sigma_\gamma - \epsilon} \Psi \qquad [38]$$

$$D\Psi = -r^{\sigma_\beta - \sigma_\varkappa} V \qquad [39]$$

Equation [37] clearly requires that $W = 0$ so that, as in the cases treated by Chandrasekhar (1961) the velocity field contains no toroidal component but is purely poloidal. The solutions for V, Ψ are most simply constructed as polynomial expansions in r. In the present analysis, this was found to be much more convenient than, for example, the Bessel function expansion of Chandrasekhar. Omitting physically unrealistic solutions which involve infinite velocities at the centre $r = 0$, it is readily verified that the solution is of the form

$$V = \sum_{k=0}^{\infty} \sum_{\ell=1}^{3} A_{k,\ell}\, r^{m_{k,\ell}} \qquad [40]$$

$$\Psi = \sum_{k=0}^{\infty} \sum_{\ell=4}^{6} A_{k,\ell}\, r^{m_{k,\ell}} \qquad [41]$$

where

$$\left.\begin{aligned} m_{k,\ell} &= \lambda_\ell + qk \\ q &= 6 + \sigma_\gamma + \sigma_\beta - \sigma_\varkappa - \epsilon \\ \lambda_1 &= n + 2 + \tau_1 \\ \lambda_2 &= n + 2 + \tau_2 \\ \lambda_3 &= n + 4 + \sigma_\gamma - \epsilon \\ \lambda_4 &= \lambda_1 + 2 - \sigma_\varkappa + \sigma_\beta \\ \lambda_5 &= \lambda_2 + 2 - \sigma_\varkappa + \sigma_\beta \\ \lambda_6 &= n \end{aligned}\right\} \qquad [42]$$

where

$$\tau_{1,2} = \frac{(1-\epsilon)}{2} + \left[n^2+n+\frac{5}{4}+\frac{\epsilon^2}{4} \pm \left[(2n+1)^2 - 3\epsilon - \epsilon^2(n^2+n-\frac{9}{4}) \right]^{\frac{1}{2}} \right]^{\frac{1}{2}} \qquad [43]$$

The coefficients $A_{k,\ell}$ follow the recursive relations

$$\frac{A_{k+1,\ell}}{A_{k,\ell}} = -n(n+1)R\left[s(s+1)-n(n+1) \right]^{-1}$$

$$\times \left[\left\{ p(p+1)-n(n+1) \right\} \left\{ (p-2)(p-1)-n(n+1)+\epsilon(2p-\epsilon-1) \right\} + 2\epsilon(\epsilon-2)(p^2-1) \right]^{-1} \qquad [44]$$

where for $\ell = 1 \rightarrow 3$, $s = m_{k,\ell}+2-\sigma_\kappa+\sigma_\beta$ and $p = m_{k,\ell}$ and for $\ell = 4 \rightarrow 6$, $s = m_{k,\ell}$ and $p = m_{k,\ell}+4+\sigma_\gamma-\epsilon$. In addition the coefficients of the first terms in the series are related as follows

$$A_{0,4} = -A_{0,1} \Big/ \left[(\lambda_1+2-\sigma_\kappa+\sigma_\beta)(\lambda_1+3-\sigma_\kappa+\sigma_\beta)-n(n+1) \right]$$

$$A_{0,5} = -A_{0,2} \Big/ \left[(\lambda_2+2-\sigma_\kappa+\sigma_\beta)(\lambda_2+3-\sigma_\kappa+\sigma_\beta)-n(n+1) \right]$$

$$A_{0,6} = A_{0,3} \frac{\left[\lambda_3(\lambda_3+1)-n(n+1) \right] \left[(\lambda_3-2)(\lambda_3-1)-n(n+1)+\epsilon(2\lambda_3-\epsilon-1) \right] + 2\epsilon(\epsilon-2)(\lambda_3^2-1)}{n(n+1)R}$$

This represents a solution to the equations [37], [38] and [39] so that, in theory, all that is left to do is to impose the three boundary conditions at the surface r = 1 in order to complete the solution. A value of unity can be assigned to one of the three remaining unknown coefficients, $A_{0,1}$, $A_{0,2}$ and $A_{0,3}$ without loss of generality. Hence two of the boundary conditions suffice to determine the other two coefficients and one condition remains which provides a relation between the Rayleigh number, R, and the other parameters, n, ϵ, σ_κ, σ_β and σ_γ (plus any that might be introduced by the boundary conditions). This relation would, in theory, serve to determine the neutrally stable value of the Rayleigh number for that choice of parameters.

However a difficulty arises which does not occur for uniformly viscous spheres. For values of ϵ which are typically less than -3 the

exponents τ_1, τ_2 and hence the rest of the solution becomes complex. A Rayleigh Number computed in the above manner would then be complex and this is not physically realistic.

The answer to this dilemma is that under such circumstances the neutrally stable state is given by solutions of the original equations [24] and [25] in which the real part of p is zero; however the imaginary part may take a non-zero value so that the solution is one which is undergoing stable oscillations in time. It is thus necessary to now examine solutions to the original equations [24] and [25].

5. Perturbation of Neutral Stability Solution to Small η.

It follows from the last section that we wish to examine solutions to the general equations by constructing perturbation solutions for small η employing, as a base, the solution of the last section. First, however, note that since ν_0 is tens of orders of magnitude greater than κ_0 in the practical situation, only the terms involving $\eta a^2/\kappa_0$ in the general equations [24] and [25] need be considered in such a solution; the terms involving $\eta a^2/\nu_0$ will be neglected. Assuming $\eta a^2/\kappa_0 < 1$, V, Ψ are considered expanded in the form

$$V = V_1 + \left(\frac{\eta a^2}{\kappa_0}\right) V_2 + O\left(\left(\frac{\eta a^2}{\kappa_0}\right)^2\right) \qquad [45]$$

$$\Psi = \Psi_1 + \left(\frac{\eta a^2}{\kappa_0}\right) \Psi_2 + O\left(\left(\frac{\eta a^2}{\kappa_0}\right)^2\right) \qquad [46]$$

where V_1, Ψ_1 are the solutions presented in the previous section. It follows from the equations [24] and [25] that V_2, Ψ_2 are given by the solution of

$$\left[D^2 + \frac{2\epsilon}{r}\frac{\partial}{\partial r} D - \frac{\epsilon(\epsilon-3)}{r^2} D - \frac{2\epsilon(\epsilon-2)}{r^2}\left\{\frac{\partial^2}{\partial r^2} + \frac{1}{r}\frac{\partial}{\partial r} - \frac{1}{r^2}\right\}\right] V_2$$

$$- n(n+1) R r^{\sigma_\gamma - \epsilon} \Psi_2 = \left(\frac{\kappa_0}{\nu_0}\right) r^{-\epsilon} DV_1 \qquad [47]$$

$$r^{\sigma_\beta - \sigma_\kappa} V_2 + D\Psi_2 = r^{-\sigma_\kappa} \Psi_1 \qquad [48]$$

Then with the use of the known solution for V, Ψ embodied in equations [40], [41], the solutions for V_2, Ψ_2 may be shown to be

$$V_2 = \sum_{k=0}^{\infty} \sum_{\ell=4}^{6} \xi_{k,\ell} A_{k,\ell} r^{m_{k,\ell}-\sigma_\beta} \qquad [49]$$

$$\Psi_2 = \sum_{k=0}^{\infty} \sum_{\ell=4}^{6} \frac{(1-\xi_{k,\ell}) A_{k,\ell} r^{m_{k,\ell}-\sigma_\kappa+2}}{\left[(m_{k,\ell}-\sigma_\kappa+2)(m_{k,\ell}-\sigma_\kappa+3)-n(n+1)\right]} \qquad [50]$$

where

$$\xi_{0,\ell} = 0$$

$$\xi_{k+1,\ell} = \frac{n(n+1)R(1-\xi_{k,\ell}) \times (A_{k,\ell}/A_{k+1,\ell})}{\left[s(s+1)-n(n+1)\right]\left[\{p(p+1)-n(n+1)\}\{(p-2)(p-1)-n(n+1)+\epsilon(2p-\epsilon-1)\}+2\epsilon(\epsilon-2)(p^2-1)\right]}$$

where $s = m_{k,\ell}-\sigma_\kappa+2$, $p = m_{k,\ell}+q-\sigma_\beta$.

It follows that the perturbed solution is

$$V = \sum_{k=0}^{\infty} \left[\sum_{\ell=1}^{3} A_{k,\ell} r^{m_{k,\ell}} + \left(\frac{\eta a^2}{\kappa_0}\right) \sum_{\ell=4}^{6} \xi_{k,\ell} A_{k,\ell} r^{m_{k,\ell}-\sigma_\beta} \right] \qquad [51]$$

$$\Psi = \sum_{k=0}^{\infty} \left[\sum_{\ell=4}^{6} A_{k,\ell} r^{m_{k,\ell}} + \left(\frac{\eta a^2}{\kappa_0}\right) \sum_{\ell=4}^{6} \frac{(1-\xi_{k,\ell}) A_{k,\ell} r^{m_{k,\ell}-\sigma_\kappa+2}}{\left[(m_{k,\ell}-\sigma_\kappa+2)(m_{k,\ell}-\sigma_\kappa+3)-n(n+1)\right]} \right] \qquad [52]$$

This then represents a solution to the general equations [24] and [25] provided $(\eta a^2/\kappa_0) \ll 1$. In addition to the prescribed parameters n, ϵ, σ_κ, σ_β and σ_γ it contains, as described previously, three unknown coefficients $A_{0,1}$, $A_{0,2}$ and $A_{0,3}$. In theory, application of three boundary conditions on the outer surface, r = 1, permits elimination of these constants to yield an explicit relation between the Rayleigh Number, R, and the growth or decay factor $(\eta a^2/\kappa_0)$; the former is a real number and, in general, results in a complex value of $(\eta a^2/\kappa_0)$, the imaginary part of which will characterize the time-harmonic nature of the growth or decay of the instability.

Consider first the solution for the case in which boundary conditions at r = 1 (section 3) are assumed to be those of a "fixed surface", that is

(i) Zero normal velocity, equation [27] gives $V = 0$ at $r = 1$

(ii) Zero tangential velocity, equation [28] gives $\frac{\partial V}{\partial r} = 0$ at $r = 1$ since $V = 0$ from condition (i)

(iii) Zero temperature perturbation gives $\Psi = 0$ at $r = 1$

Using the relations [51], [52] and [44] each of these conditions yields an equation of the form

$$\sum_{\ell=1}^{3} A_{0,\ell} \; B_\ell + \left(\frac{\eta a^2}{\kappa_0}\right) \sum_{\ell=1}^{3} A_{0,\ell} \; C_\ell = 0 \qquad [53]$$

where for a given Rayleigh number the coefficients B_ℓ and C_ℓ can be explicitly computed for each of the three conditions. Finally, the value of $(\eta a^2/\kappa_0)$ -- that is to say the growth or decay parameter for the particular value of R prescribed -- can be calculated from the condition that the determinant of the coefficients of $A_{0,\ell}$ in the equations must be zero. Neglecting all terms quadratic (or higher) in $(\eta a^2/\kappa_0)$ allows a direct calculation of $(\eta a^2/\kappa_0)$. All of this was accomplished by a computer program which required as input n, ϵ, σ_κ, σ_β, σ_γ and R and produced values of the real and imaginary parts of $(\eta a^2/\kappa_0)$. Consequently a search was performed to locate the particular values of R which yielded a $(\eta a^2/\kappa_0)$ with a zero real part; this is the neutrally stable or critical value of R for a given set of the other parameters.

Clearly different boundary conditions required only minor changes to such a program. For example the classical free surface solution requires only a substitution of the zero tangential stress condition (which from [31] becomes $\partial^2 V/\partial r^2 = 0$ at $r = 1$) for the zero tangential velocity condition, and the consequent changes in the coefficients B_ℓ, C_ℓ in one of the equations [53]. The resulting critical Rayleigh numbers in this case are displayed in Figure 3 for parametric values $\sigma_\kappa = \sigma_\beta = \sigma_\gamma = 0$. A check on the solution was provided by comparison of the results for the uniformly viscous case, $\epsilon = 0$, with the results of Chandrasekhar (1961); they are identical to four significant figures. For the cases $\epsilon = -5, -10, -20$ the neutral stability values of the imaginary part of $(\eta a^2/\kappa_0)$ were also obtained. Enthusiasm for intriguing possibility of stable or near stable oscillatory solutions was dispelled when

values of this quantity were found to be less than 10^{-4} for all cases examined including those with positive amplification rates. This would involve a period of the order of 10^{16} years in the case of the earth's mantle, a figure many orders of magnitude greater than the lifetime of the earth (order 5×10^{9} years).

The results of Figure 3 and similar data for the rigid outer boundary case show predictably greater critical surface Rayleigh numbers as the rate of increase of viscosity with depth increases. The value of the surface Rayleigh number for the earth's mantle in its present state is roughly 10^{10} based on reasonable choices of $\alpha_0 = 2 \times 10^{-5}\ (°K)^{-1}$, $\varkappa_0 = 3 \times 10^{-2}\ cm^2/sec$, $2\beta_0 a = 1.5 \times 10^{-5}\ °K/cm$, $a = 6,37 \times 10^{8}$ cm, ρ(density) = 3.7 gm/cm^3 and $\mu_0 = 0.6 \times 10^{21}$ poise taken from Knopoff (1964), Birch (1964), Clark (1957), Bullard (1954), Turcotte and Oxburgh (1969), Brennen (1973) and other sources. Thus even with the most extreme choice of the viscosity increase factor, ε, the earths mantle would still appear to be far beyond the neutrally stable state envisaged in some of the early work. A further result of the present calculation seems to confirm this conclusion beyond doubt. Computation of the amplification factor (real and positive parts of $\eta a^2/\varkappa_0$ indicates that close to the neutral stability solution the rate of change of $\eta a^2/\varkappa_0$ with R has a maximum value of order 10^{-4}. Thus, for example, the typical growth time, $1/\eta$, corresponding to a deviation from the neutral stability position of 100% in Rayleigh number is of the order of $10^{11 \to 13}$ years. It follows that the earth's mantle must have been in a much more highly unstable state in order for the present convective pattern to have established itself; this is consistent with the highly supercritical value of $R \cong 10^{10}$ for the mantle. Unfortunately it also follows that the preceding calculation like those of Chandrasekhar (1961) is of very little use in constructing a history for the growth of the present mantle convection pattern. This is illustrated in the next section where we proceed to develop a method for calculating initial growth rates in cases of highly supercritical Rayleigh number.

6. Growth of Supercritical Convective Instabilities in the Earth's Mantle

Consideration of the magnitude of the parameters $\eta a^2/\kappa_0$ and $\eta a^2/\nu_0$ in the basic equations [24] and [25] rapidly leads to the conclusion that as far as thermal convective instability in the earth's mantle is concerned, the region of interest is described by

$$\eta a^2/\kappa_0 \gg 1 \quad , \quad \eta a^2/\nu_0 \ll 1 \qquad [54]$$

This is readily demonstrated by noting that the typical growth time, η^{-1}, corresponding to $\eta a^2/\kappa_0 = 1$ is 10^{12} years which is three orders of magnitude greater than the lifetime of the earth. Hence for all instabilities of interest $\eta a^2/\kappa_0 \gg 1$. Further $\eta a^2/\nu_0 = 1$ when $\eta^{-1} \cong 10^{-11}$ years; hence all instabilities of interest have $\eta a^2/\nu_0 \ll 1$.

But the neutral stability solutions described by Chandrasekhar (1961) and employed in the last section can clearly only be considered to have any validity when both $\eta a^2/\nu_0$ and $\eta a^2/\kappa_0$ are very much less than unity; indeed the former are restricted to $\eta = 0$. The thesis of the present paper is that solutions appropriate to the instability in the mantle must be calculated under the conditions, [54], which are fundamentally different. Indeed it transpires that supercritical calculations within the ranges described by [54] may be made more readily than those for neutral stability. When $\eta a^2/\kappa_0 \gg 1$, $\eta a^2/\nu_0 \ll 1$ the basic equations [23], [24] and [25] can clearly be simplified to

$$\left[D + \frac{\varepsilon}{r}\frac{\partial}{\partial r} - \frac{\varepsilon}{r^2}\right] W(r) = 0 \qquad [55]$$

$$\left[D^2 + \frac{2\varepsilon}{r}\frac{\partial}{\partial r} D - \frac{\varepsilon(\varepsilon-3)D}{r^2} + \frac{2\varepsilon(\varepsilon-2)}{r^2}\left\{\frac{\partial^2}{\partial r^2} + \frac{1}{r}\frac{\partial}{\partial r} - \frac{1}{r^2}\right\}\right] V(r)$$

$$= n(n+1) R\, r^{\sigma_\gamma - \varepsilon}\, \Psi(r) \qquad [56]$$

$$\left(\frac{\eta a^2}{\kappa_0}\right)\Psi(r) = r^{\sigma_\beta}\, V(r) \qquad [57]$$

As before, the solution to [55] remains $W = 0$. However the function $\Psi(r)$ may now be eliminated from [56] and [57] to yield the following equation for $V(r)$:

$$\left[D^2+\frac{2\epsilon}{r}\frac{\partial}{\partial r}D-\frac{\epsilon(\epsilon-3)}{r^2}+\frac{2\epsilon(\epsilon-2)}{r^2}\left\{\frac{\partial^2}{\partial r^2}+\frac{1}{r}\frac{\partial}{\partial r}-\frac{1}{r^2}\right\}-n(n+1)\left(\frac{R\varkappa_0}{\eta a^2}\right)r^{\sigma_\gamma+\sigma_\beta-\epsilon}\right]V=0 \quad [58]$$

In terms of the variables employed in the last section the series solution to this equation is simply

$$V(r)=V^*r^{n+2}\left[\begin{array}{l} r^{\tau_1}+G(\tau_3)\left(\frac{R\varkappa_0}{\eta a^2}\right)r^{\tau_3}+G(\tau_3)G(r_5)\left(\frac{R\varkappa_0}{\eta a^2}\right)^2 r^{\tau_5}+\cdots \\ \\ +B\left\{r^{\tau_2}+G(\tau_4)\left(\frac{R\varkappa_0}{\eta a^2}\right)r^{\tau_4}+G(\tau_4)G(\tau_6)\left(\frac{R\varkappa_0}{\eta a^2}\right)^2 r^{\tau_6}+\cdots\right\}\end{array}\right] \quad [59]$$

where V^* and B are arbitrary constants, τ_1, τ_2 are given, as before, by the relation [43] and

$$\tau_k=\tau_{k-2}+\sigma_\gamma+\sigma_\beta-\epsilon+4$$

$$G(\tau)=n(n+1)\Big/\left[\begin{array}{c}\left\{\tau(\tau+1)-n(n+1)\right\}\left\{(\tau-2)(\tau-1)-n(n+1)+\epsilon(2\tau-\epsilon-1)\right\} \\ +2\epsilon(\epsilon-2)(\tau^2-1)\end{array}\right]$$

The temperature profile Ψ is readily obtained from equation [57].

Consider now the application of boundary conditions. In this construction application of the condition $V=0$ at $r=1$ automatically satisfies the temperature condition $\Psi=0$ at $r=1$ because of the relation [57]. If we then choose to examine the case of a 'free' boundary at $r=1$ the conditions $V=0$ and $\partial^2V/\partial r^2=0$ substituted into [59] lead to the two equations

$$1+G(\tau_3)\left(\frac{R\varkappa_0}{\eta a^2}\right)+G(\tau_3)G(\tau_5)\left(\frac{R\varkappa_0}{\eta a^2}\right)^2+\cdots$$

$$+B\left\{1+G(\tau_4)\left(\frac{R\varkappa_0}{\eta a^2}\right)+G(\tau_4)G(\tau_6)\left(\frac{R\varkappa_0}{\eta a^2}\right)^2+\cdots\right\}=0 \quad [60]$$

$$H(\tau_1)+H(\tau_3)G(\tau_3)\left(\frac{R\varkappa_0}{\eta a^2}\right)+H(\tau_5)G(\tau_3)G(\tau_5)\left(\frac{R\varkappa_0}{\eta a^2}\right)^2+\cdots$$

$$+B\left\{H(\tau_2)+H(\tau_4)G(\tau_4)\left(\frac{R\varkappa_0}{\eta a^2}\right)+H(\tau_6)G(\tau_4)G(\tau_6)\left(\frac{R\varkappa_0}{\eta a^2}\right)^2+\cdots\right\}=0 \qquad [61]$$

where $H(\tau)=(\tau+n+2)(\tau+n+1)$. Elimination of B yields a single equation which may be solved to yield a value for $R\varkappa_0/\eta a^2$. This requires that the series in equations [60] and [61] converge and despite values of $R\varkappa_0/\eta a^2 \gg 1$ such convergence almost invariably occurs because of the nature of the function $G(\tau)$. As in the solution of section 5 the values of τ become complex below a value of ϵ of about -3 and therefore, in general, the resulting value of $R\varkappa_0/\eta a^2$ also becomes complex. This in turn yields a complex value of η the imaginary part of which corresponds to the oscillatory nature of the growth of the instability.

Computed values of the real part of $R\varkappa_0/\eta a^2$ are displayed in figure 4 for both the free outer boundary and the rigid outer boundary ($V=0$, $\partial V/\partial r$ at $r=1$) cases. Both of these computations have employed $\sigma_\varkappa=\sigma_\beta=\sigma_\gamma=0$. However other values of these secondary parameters are also of interest. In this regard it should be noted that $\sigma_\varkappa$ does not appear in the solution and that σ_β, σ_γ only occur in the combination $\sigma_\beta+\sigma_\gamma$ ($=\sigma$, say). Thus a solution with a particular value of σ corresponds to a wide range of physically different examples. Figure 5 displays the results of the free boundary cases with $\sigma=-1$ and $\sigma=-3$, in contrast to the $\sigma=0$ of figure 4. With reference to the earth's mantle it should be noted that $\sigma_\gamma=0$ corresponds to the case of constant g within the mantle (α being assumed constant) and it appears that this is a reasonably valid approximation. The case of constant rg which Chandrasekhar mentions corresponds to $\sigma_\gamma=-1$ (and thus $\sigma=-1$ if $\sigma_\beta=0$). When $\sigma_\beta=0$ the temperature gradient given by equation 4 pertains to a uniform distribution of heat sources within the sphere. Negative values imply a concentration of sources closer to the center of the sphere. Hence the case $\sigma_\beta=-1$, Figure 5, may be somewhat more realistic than $\sigma=0$ in so far as the earth's mantle is concerned, though the results of the two calculations do not differ greatly. The case $\sigma_\beta=-3$

corresponds to the absence of heat sources except for the center of the sphere. It seems unlikely that the conditions existing in the mantle would lie outside the range of σ investigated.

Figures 4 and 5 allow simple calculation of the incipient growth rate for thermal convection or, alternately, the typical time for development of a new pattern arising because of changing conditions. Assuming, for example, a value of 10^{10} for the surface Rayleigh number, R, figure 5 shows that the response time, η^{-1}, for the degree $n = 3$ instability with $\sigma = -1$ is 1.5×10^4, 4.4×10^4, 18.0×10^4 and 103×10^4 years for $\varepsilon = 0$, -2, -5 and -10 respectively. Thus the growth and response times indicated for thermal convection in the mantle are quite rapid by geological standards; uncertainty in the Rayleigh number of about an order of magnitude should, however, be noted in forming any definite conclusion.

As was the case with the results of section 5 the imaginary parts of $R\varkappa_0/\eta a^2$ which were calculated led to values of the imaginary part of η which were very small. Indeed the smallest period calculated for the oscillatory component was of order 10^{11} years (with $R = 10^{10}$) and by comparison with the response times it seems clear that this feature of the motion is negligible.

The minimums exhibited by the curves in Figures 4 and 5 are of particular interest in view of the convection pattern existing at the present time since this appears to contain predominant harmonics of degree 3 or 4. Examination of the figures suggests that this should only be the case if the increase of viscosity with depth were given approximately by $\varepsilon = -2$. This corresponds to a rather small increase in which the viscosity of the lower mantle is about 4 times that on the upper mantle boundary. It is not, however, out of line with the recent theoretical studies of Weertman (1970) and agrees well with that suggested by Brennen (1973) from a reexamination of isostatic recovery data in the light of Weertman's theory and with values of $10^{22} \rightarrow 10^{24}$ poise proposed by both Dicke (1969) and Goldreich and Toomre (1969) for the lower mantle. The corresponding response times of the order of 10^5 years appear in siginficant disagreement with the "memory" of 10^7 years employed by Macdonald (1963, 1965), Kaula (1967) in order to explain polar wandering on the basis of lower mantle viscosity (which equivalently is required to be of order 10^{26} poise). This latter theory is however growing in disfavor (Goldreich and Toomre (1969)) and shorter response times or memories would appear to be indicated.

7. Pattern of Incipient Convective Flow

In order to display the patterns of incipient convective flow it is necessary to construct from the solution for V(r) the relations for the velocity components v_r, v_θ, v_Φ in the three spherical coordinate directions. It is readily established from equation [11], the equation of continuity and the condition W = 0 that:

$$v_r = \frac{V}{r} S_n(\theta,\varphi)\, \ell^{\eta t} \qquad [62]$$

$$v_\theta = \left[\frac{1}{r}\frac{\partial}{\partial r}(rV)\right] \frac{\partial S_n}{\partial \theta} \frac{\ell^{\eta t}}{n(n+1)} \qquad [63]$$

$$v_\Phi = \left[\frac{1}{r}\frac{\partial}{\partial r}(rV)\right] \frac{1}{\sin\theta} \frac{\partial S_n}{\partial \Phi} \frac{\ell^{\eta t}}{n(n+1)} \qquad [64]$$

Then the choice of a particular spherical harmonic function, S_n, is all that is required in order to evaluate the relative magnitude and directions of the velocity vector for the incipient flow within the sphere.

This is illustrated by the choice of $S_n = \cos(\lambda\varphi) P_n^\lambda(\cos\theta)$ in figures 6, 7, and 8; here we have set $\lambda = 0$ and $n = 3$ so that the component $v_\Phi = 0$. Figure 6 illustrates the relative magnitudes and directions of the surface velocities for the free surface solution of section 6; since this involves only v_θ and represents only relative surface velocities the figure is independent of the parameters ϵ and σ. It is superimposed on a world map by selecting the positions 85°E, 10°N and 95°W, 10°S for the poles of the convection pattern. The choice of this example was designed for comparison with the inferred convective patterns in the earth's mantle shown in Figures 1 and 2. Though the comparison with Runcorn's data is more satisfactory than with that from sea floor spreading it would still seem reasonable to conclude that the n = 3 harmonic is a substantial component in the mantle convection pattern. Indeed significant improvement in the correlation may be obtained by the addition of n = 3 components with $\lambda = 1, 2$, etc.

Figures 7 and 8 present the flow field in the cross-sectional plane through the poles of the convection pattern. Only the quadrant $\theta = 0$ to $\frac{\pi}{2}$ is shown since the pattern is antisymmetric about $\theta = \frac{\pi}{2}$ and symmetric about $\theta = 0, \pi$. Figure 8 displays the flow field for the uniformly viscous case

$\epsilon = 0$, $\sigma = 0$ of the free surface solution of section 6 . In contrast, figure 9 shows a similar solution for a sphere with substantial increase of viscosity with depth given by $\epsilon = -5$. The relative decrease of the velocities closer to the sphere center (or equivalently the increase of the surface velocities) is clearly seen; the cell center also moves significantly closer to the surface. It is not difficult to envisage a mantle convection pattern quite similar to that of figure 8. The relative velocities at $r = \frac{1}{2}$ are sufficiently small so that the substitution of a lower mantle boundary at a depth of about 3000 km. could reasonably be expected to cause little alteration in the convection flow pattern. It should however be stressed again that these are incipient flow patterns indicated by the analysis; the resulting fully developed convective flow may depart significantly from this pattern.

8. True Free Surface Condition with Surface Distortion

In the preceding sections it was tacitly assumed that the "free boundary" solution developed there was pertinent to the studies of convection in the earth's mantle. Such a solution is analogous to the asymptotic case of zero Froude number in water wave problems. In this section we shall investigate the effect of a more general application of the true linearized free surface conditions derived in section 3.

Toward this end the boundary conditions of section 5 should be replaced by the shear stress condition [31] and the normal stress condition [36] with W set equal to zero. Since the term involving $\eta a^2/\nu_0$ on the right hand side is negligible, the normal stress condition can be manipulated to read

$$\left(\frac{R\varkappa_0}{\eta a^2}\right) n(n+1) V = 2\beta\alpha a^2 \left[\frac{\partial}{\partial r}\left\{r\,DV - \frac{2n(n+1)}{r}\right\} - \epsilon\, DV\right] \qquad [65]$$

on $r = 1$. It is particularly significant to note that the gravitational component of the coefficient of the right hand side has been absorbed into the $(R\varkappa_0/\eta a^2)$ on the left. Thus the dimensionless quantity $M = 2\beta\alpha a^2$ which is analogous to a Froude number does not actually contain g. When $M \to 0$ the conditions revert to those of the "free boundary" employed in the preceding sections ($V = 0$, $\partial^2 V/\partial r^2 = 0$ on $r = 1$).

A solution similar to that of section 5 but utilizing the true free surface conditions [31] and [65] may be readily constructed. Results of

such calculations are shown in figure 9 for $\sigma = 0$ and various values of ϵ, n and M. It is clear that values of M substantially greater than unity would be required before the results deviated significantly from those of M = 0, figures 4 and 5 The value of M for the earth's mantle is about 0. 2; hence the assumption of the M = 0 yields little error in this case. There may, however, be other planetary bodies in which this "zero Froude number" approximation is not valid and recourse should be made to solutions of the type developed in this section.

9. Concluding Remarks

This paper has been concerned primarily with the thermal convective instabilities of a non-uniformly viscous liquid sphere heated from within. Two characteristically different solutions are presented. The first involves an extension of the classic problem of a uniformly viscous sphere (Chandrasekhar (1961)) to cover (1) the case of radial variation of viscosity and (2) cases of near critical Rayleigh number. The latter analysis provides an indication of the convection flow growth rates for Rayleigh numbers marginally greater than the critical value. The second solution is relevant to highly supercritical Rayleigh numbers and permits evaluation of the incipient growth rates under such circumstances. Results are presented for different radial variations of viscosity as well as body force (gravity) and heat sources. The most unstable mode in terms of the degree, n, of the predominant spherical harmonic in the resulting flow changes with the magnitude of the radial variation of viscosity.

Different boundary conditions on the outer surface of the sphere are also explored including the classical "free" and "fixed" conditions. A parenthetical section (section 8) is added in order to investigate the effect of a true free surface condition which permits distortion of the outer spherical boundary. Predictably this requires the specification of an additional parameter, $M = 2\beta\alpha a^2$, which is somewhat analogous to a Froude number in its effect. Though the value of M for the earth and its mantle is too small to yield substantial difference with the classic "free" boundary results (M = 0) there may be other planetary bodies for which this effect is important.

Application of the results of these calculations to the stability of the earth's mantle must be made with cognizance of other mantle features which may influence its stability and are not included in the analysis, such as chemical differentiation (Elsasser (1971, 1972)). Nevertheless such application yields some interesting results. First the growth times, η^{-1}, computed from the marginally stable solutions are considerably larger than the lifetime of the earth, indicating that the existing convection patterns must have arisen from highly supercritical conditions and Rayleigh numbers. Indeed it is easily demonstrated that relevant solutions should require $\eta\kappa_o/a^2 \gg 1$ and $\eta\nu_o/a^2 \ll 1$ and the supercritical solutions of section 6 are designed for use in this regime. For an estimated mantle Rayleigh number of the order of 10^{10} the latter calculations yield growth times of the order of 10^5 years which does not appear totally unreasonable. They also suggest that the present convection pattern in which the spherical harmonic of degree 3 predominates would be the most unstable mode if the radial variation of viscosity were roughly like r^{-2}. This would correspond to a deep mantle viscosity some 4 times the upper mantle value. Such a conclusion appears consistent with more recent views of the variation of viscosity within the earth's mantle (Weertman (1970), Brennen (1973)).

References

[1] Birch, F. 1964. Density and composition of mantle and core. J. Geophys. Res., Vol. 69, No. 20, pp. 4377 - 4388.

[2] Brennen, C. 1973. Isostatic recovery and the strain rate dependent viscosity of the earth's mantle. Submitted for publication.

[3] Bullard, E. 1954. The interior of the earth. In "The Earth as a Planet. Volume II. The solar system" edited by G. P. Kuiper, the University of Chicago Press, Chicago, pp. 57 - 137.

[4] Chandrasekhar, S. 1961. Hydrodynamic and hydromagnetic stability. Clarendon Press, Oxford, England.

[5] Clark, S. P. 1957. Radiative transfer in the earth's mantle. Trans. Amer. Geophys. Union, Vol. 38, pp. 931 - 938.

[6] Dicke, R. H. 1969. Average acceleration of the earth's rotation and the viscosity of the deep mantle. J. Geophys. Res., Vol. 74, pp. 5895 - 5902.

[7] Elsasser, E. M. 1971. Two-layer model of upper-mantle circulation. J. Geophys. Res., Vol. 76, pp. 4744 - 4753.

[8] Elsasser, W. M. 1972. Viscous statification of the earth and convection. Physics of the Earth and Planetary Interior, Vol. 6, No. 1 - 3, p. 198 - 204.

[9] Goldreich, P. and Toomre, A. 1969. Some remarks on polar wandering. J. Geophys. Res., Vol. 74, p. 2555.

[10] Heiskanen, W. A. and Vening Meinesz, F. A. 1958. The Earth and its gravity field. McGraw-Hill, New York.

[11] Kaula, W. M. 1967. Geophysical implications of satellite determinations of the earth's gravitational field. Space Sci. Rev., Vol. 7, pp. 769 - 794.

[12] Knopoff, L. 1964. The convection current hypothesis. Rev. Geophys., Vol. 2, pp. 89 - 122.

[13] Macdonald, G. J. F. 1963. The internal constitutions of the inner planets and the moon. Space Sci. Rev., Vol. 2, p. 274.

[14] Macdonald, G. J. F. 1965. The figure and long-term mechanical properties of the earth, in "Advances in Earth Science" (ed. P. M. Hurley), M. I. T. Press, Cambridge. Mass., pp. 199 - 245.

[15] McConnell, R. K. 1968. Viscosity of the mantle from relaxation time spectra of isostatic adjustment. J. Geophys. Res., Vol. 73, No. 33, pp. 7089 - 7105.

[16] Milne Thomson, L. M. 1968. Theoretical Hydrodynamics. Fifth Edition, The Macmillan Company, New York.

[17] Runcorn, S. K. 1964. Satellite gravity measurements and a laminar viscous flow model of the Earth's mantle. J. Geophys. Res., Vol. 69, No. 20, pp. 4389 - 4394.

[18] Takeuchi, H. and Sakata, S. 1970. Convection in a mantle with variable viscosity. J. Geophys. Res., Vol. 75, No. 5, pp. 921 - 927.

[19] Turcotte, D. L. and Oxburgh, E. R. 1967. Finite amplitude convective cells and continental drift. J. Fluid Mech., Vol. 28, Part 1, pp. 29 - 42.

[20] Turcotte, D. L. and Oxburgh, E. R. 1969. Convection in a mantle with variable physical properties. J. Geophys. Res., Vol. 74, pp. 1458 - 1474.

[21] Weertman, J. 1970. The creep strength of the earth's mantle. Rev. Geophys. Res., Vol. 8, pp. 145 - 168.

[22] Wilson, J. T., et al 1971. Continents Adrift. Readings from Scientific American with introduction by J. Tuzo Wilson. W. H. Freeman and Company, San Francisco.

Figure Captions

Figure 1. Surface motions (⟶) created by convection currents in the earth's mantle as inferred from studies of ocean floor spreading and continental drift. In this construction taken from Wilson(1971) mid-ocean ridges (—┆—) coincide with regions of upwelling and deep ocean trenches, island arcs, recent mountain belts and areas of deep earthquakes (||||||||||||) reflect downwelling.

Figure 2. Surface motions created by convection currents as inferred by Runcorn(1964) from anomalies in the earth's gravitational field. Arrows represent relative magnitude and direction of the surface velocity vector.

Figure 3. Critical Rayleigh numbers for the case of a free outer boundary (with $\sigma_\alpha = \sigma_\beta = \sigma_\gamma = 0$) as a function of spherical harmonic degree n for various values of the rate of increase of viscosity with depth represented by ϵ.

Figure 4. Results of the supercritical thermal convection growth rate calculation for $\sigma = 0$, various values of the parameter ϵ representing the increase of viscosity with depth and for the cases of an outer free boundary (———) and an outer fixed boundary (-------).

Figure 5. Results of the supercritical thermal convection growth rate calculation for an outer free boundary with $\sigma = -1$ and $\sigma = -3$ and various values of the parameter ϵ representing the increase of viscosity with depth.

Figure 6. Relative magnitudes and directions of the surface velocities for an incipient convection pattern of degree 3 superimposed on a world map by selecting the points 85°E, 10°N and 95°W, 10°S as convection poles.

Figure 7. Relative magnitudes and directions of the fluid velocities in a cross-sectional plane from the incipient growth rate solution for $n = 3$ with an outer free boundary, $\sigma = 0$ and uniform viscosity ($\epsilon = 0$).

Figure 8. Relative magnitudes and directions of the fluid velocities in a cross-sectional plane from the incipient growth rate solution for $n = 3$ with an outer free boundary, $\sigma = 0$ and a viscosity which increases with depth according to $\epsilon = -5$.

Figure 9. Results of the supercritical thermal convection growth rate calculation with a true free surface condition and various values of ϵ representing the increase of viscosity with depth and parameter $M = 2\beta\alpha a^2$.

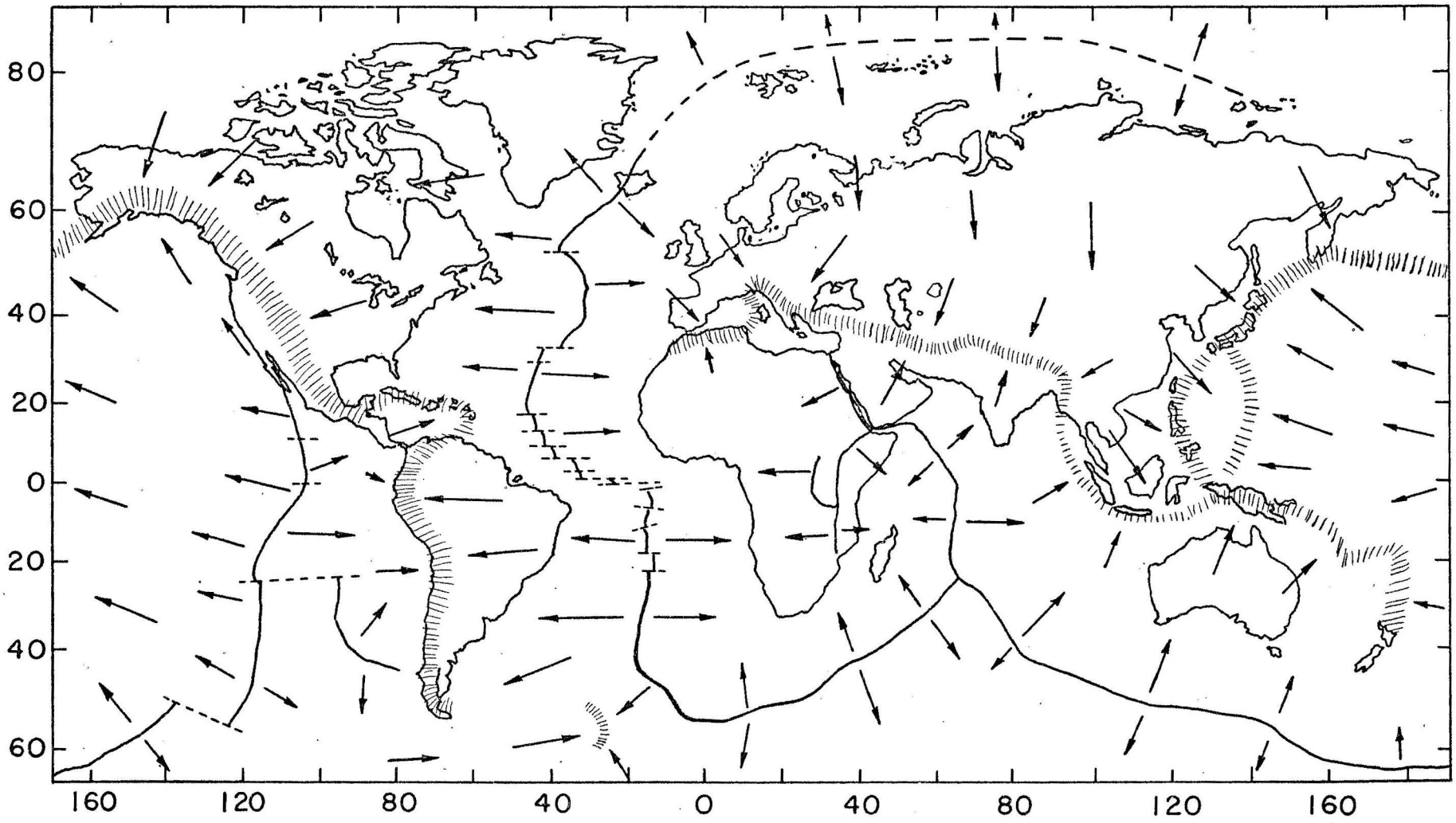

Figure 1. Surface motions (⟶) created by convection currents in the earth's mantle as inferred from studies of ocean floor spreading and continental drift. In this construction taken from Wilson(1971) mid-ocean ridges (—┼—) coincide with regions of upwelling and deep ocean trenches, island arcs, recent mountain belts and areas of deep earthquakes (▥) reflect downwelling.

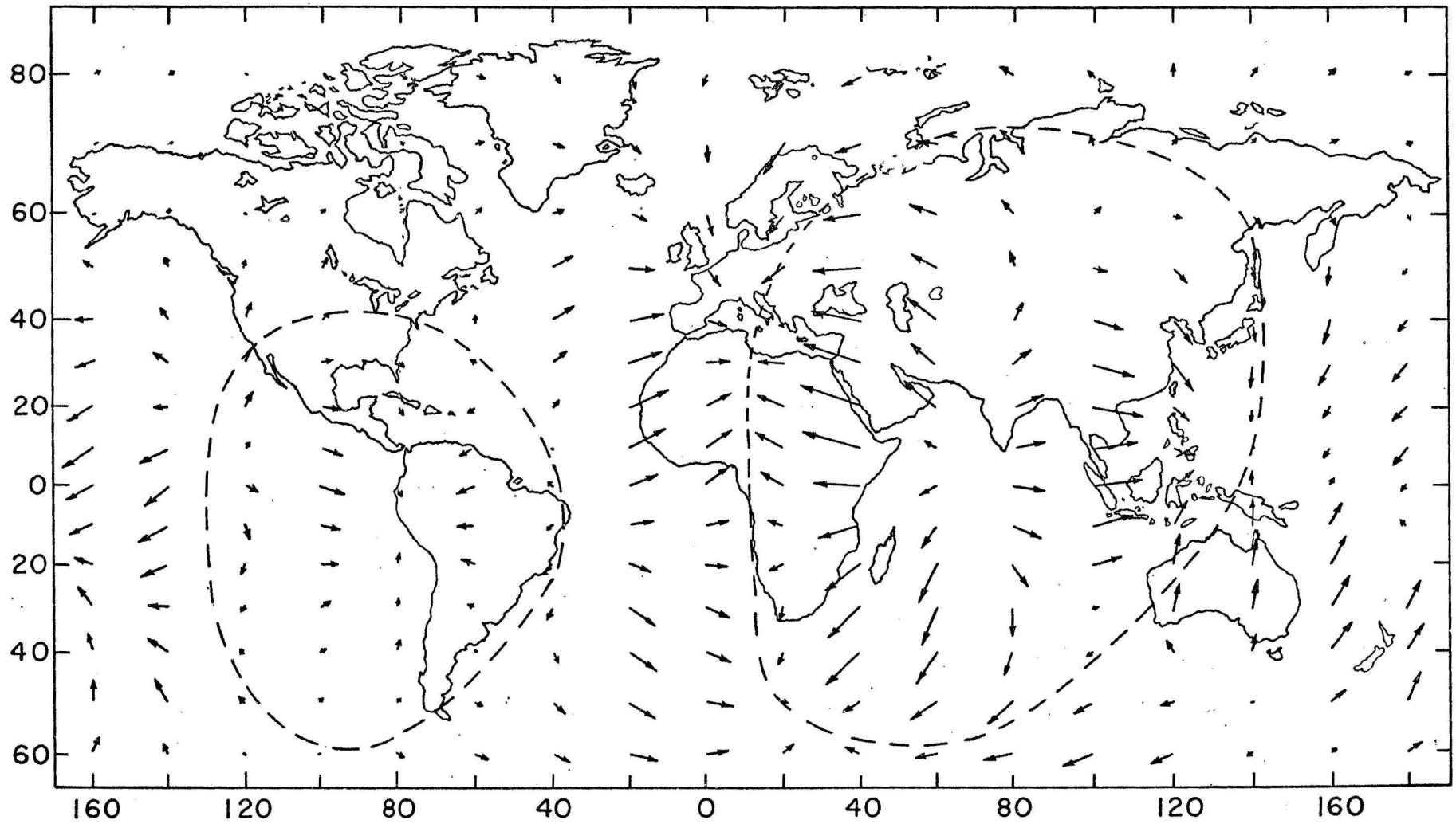

Figure 2. Surface motions created by convection currents as inferred by Runcorn(1964) from anomalies in the earth's gravitational field. Arrows represent relative magnitude and direction of the surface velocity vector.

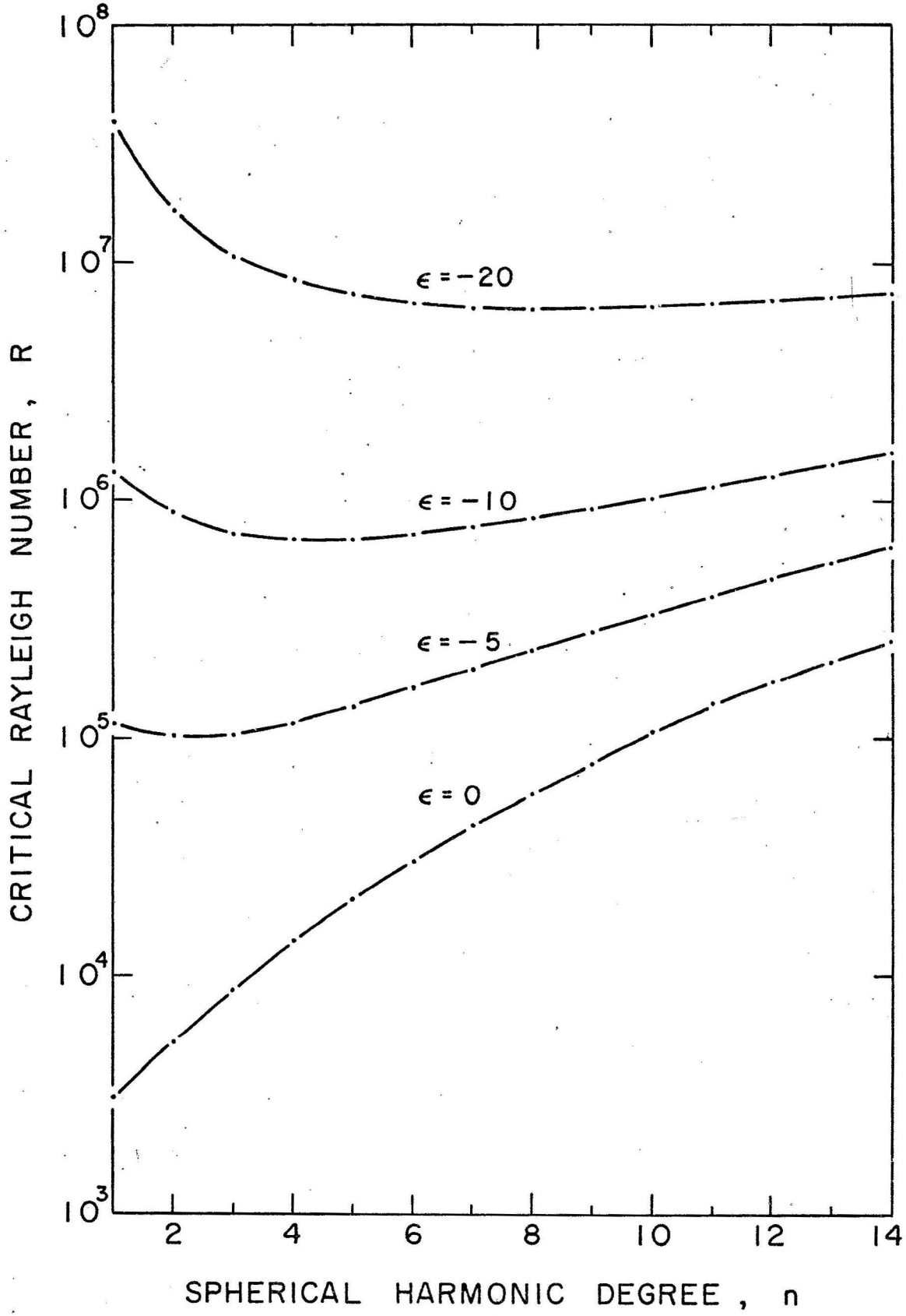

Figure 3. Critical Rayleigh numbers for the case of a free outer boundary (with $\sigma_\alpha = \sigma_\beta = \sigma_\gamma = 0$) as a function of spherical harmonic degree n for various values of the rate of increase of viscosity with depth represented by ϵ.

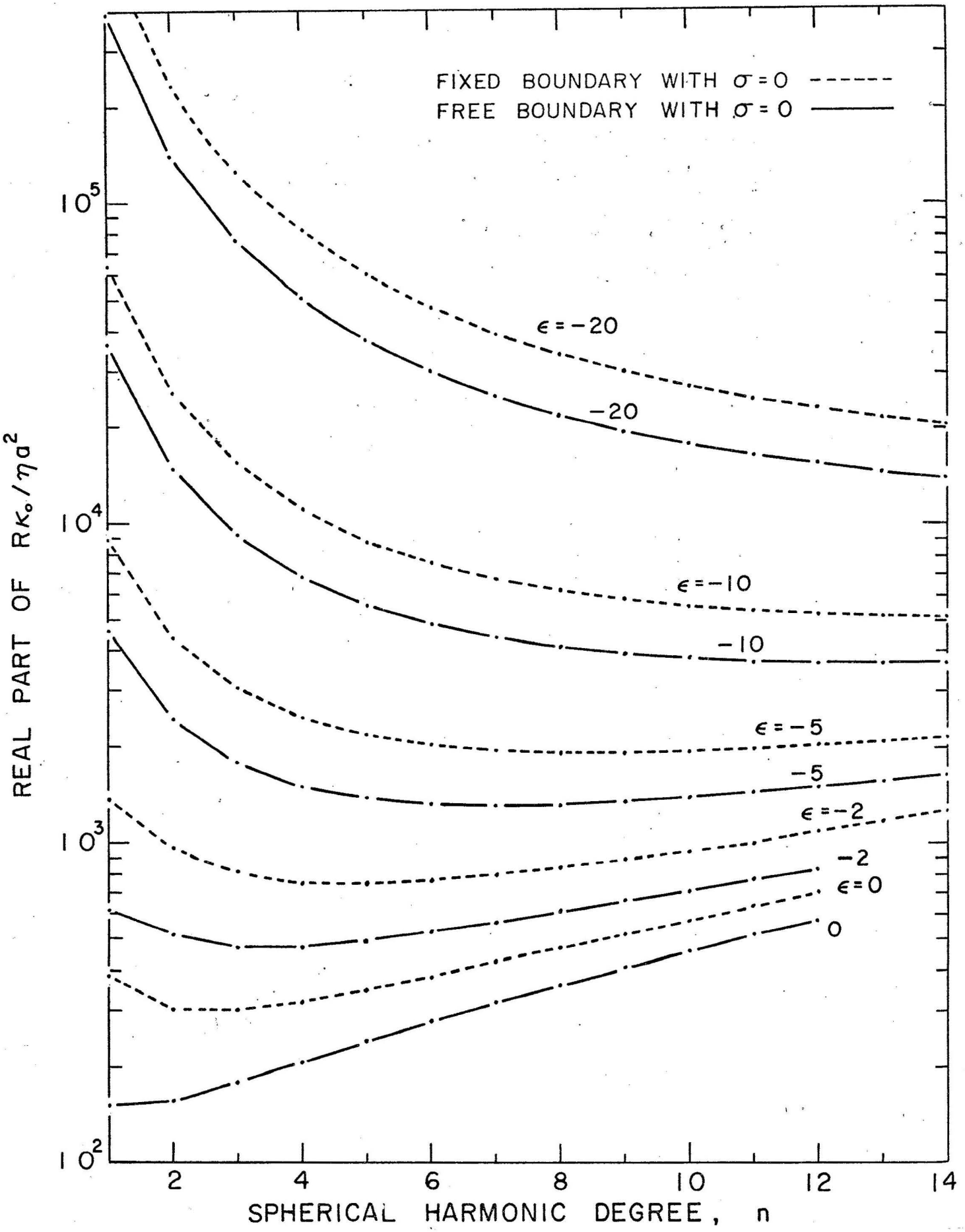

Figure 4. Results of the supercritical thermal convection growth rate calculation for $\sigma = 0$, various values of the parameter ϵ representing the increase of viscosity with depth and for the cases of an outer free boundary (_____) and

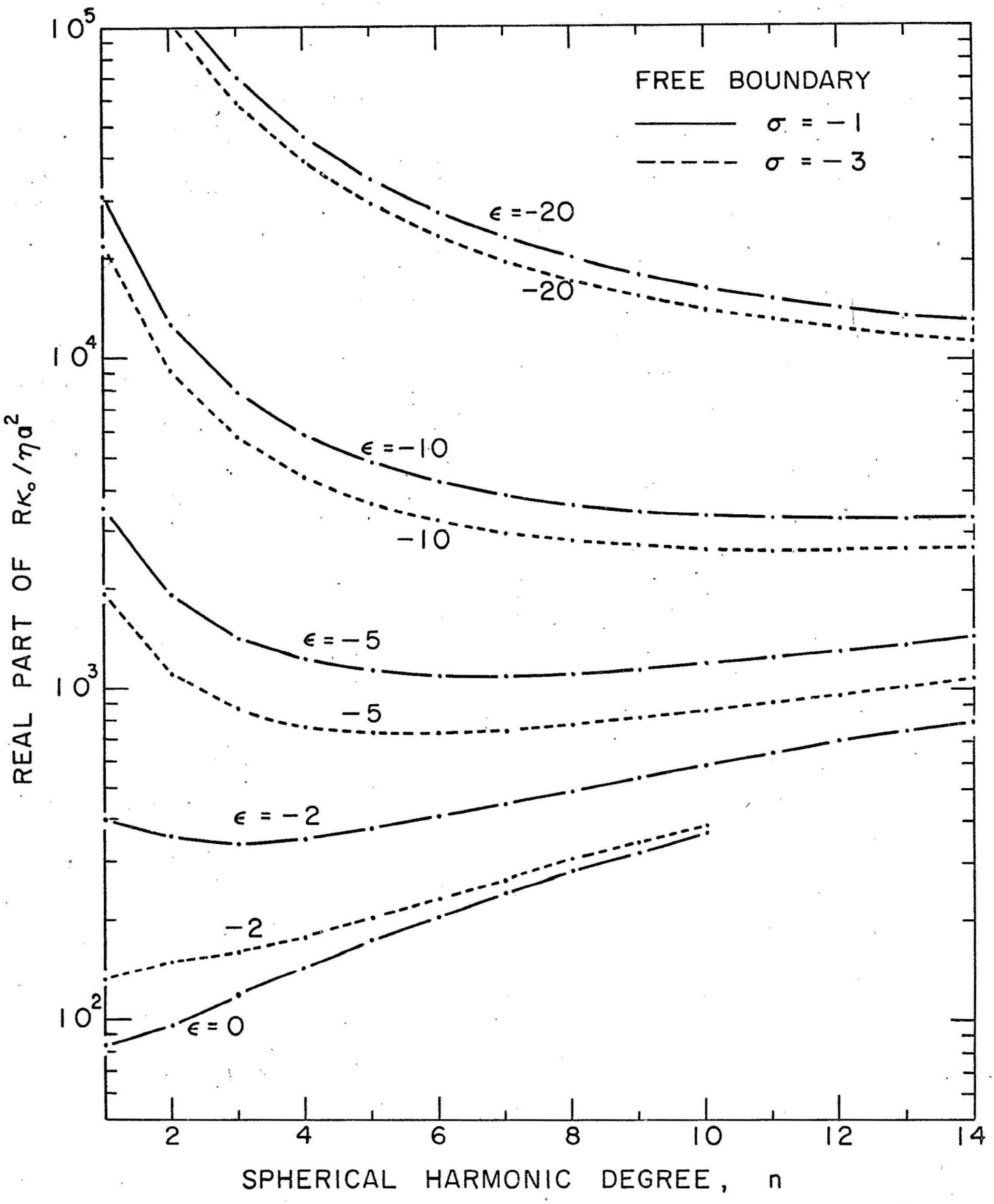

Figure 5. Results of the supercritical thermal convection growth rate calculation for an outer free boundary with $\sigma = -1$ and $\sigma = -3$ and various values of the parameter ϵ representing the increase of viscosity with depth.

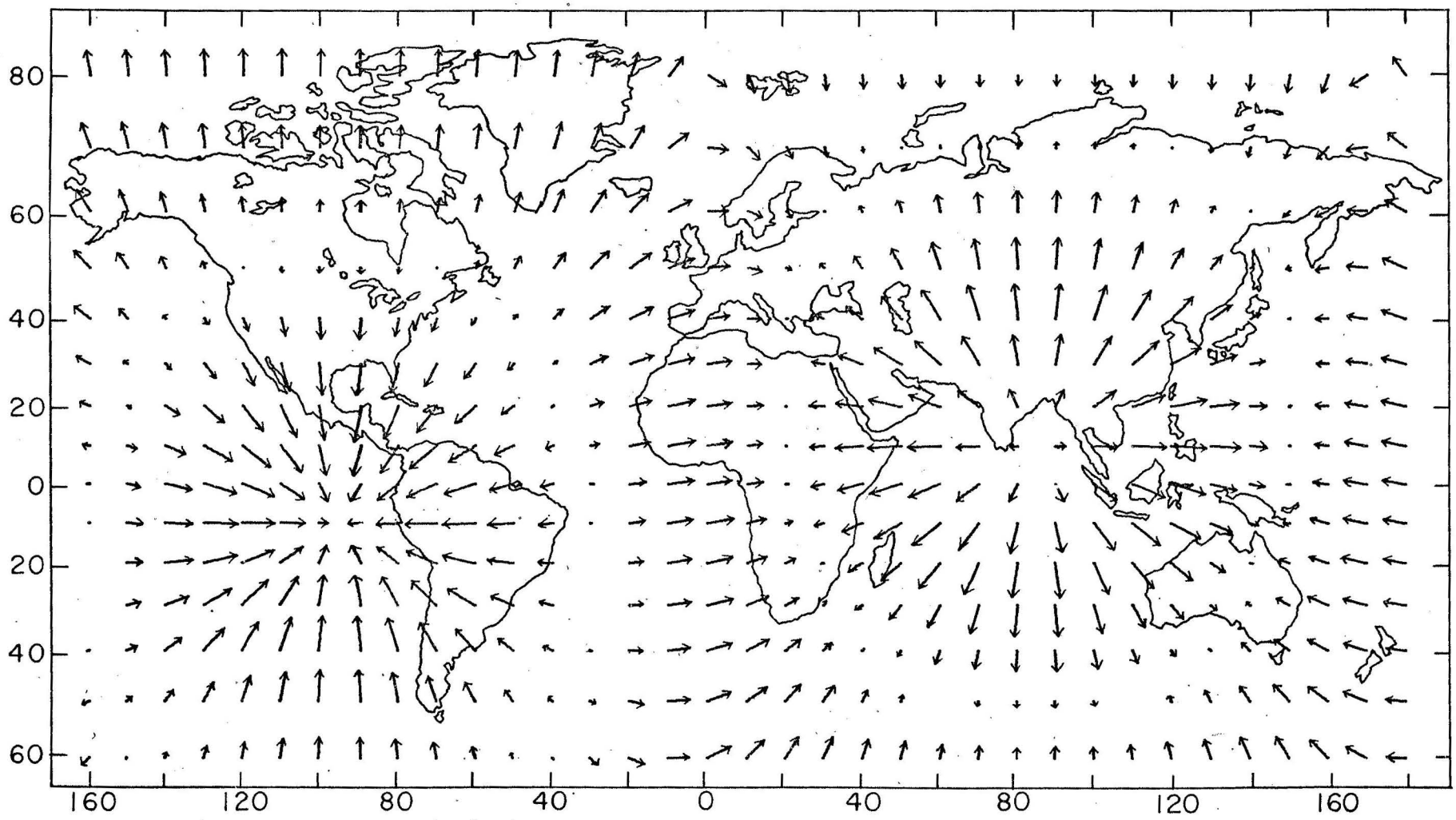

Figure 6. Relative magnitudes and directions of the surface velocities for an incipient convection pattern of degree 3 superimposed on a world map by selecting the points 85°E, 10°N and 95°W, 10°S as convection poles.

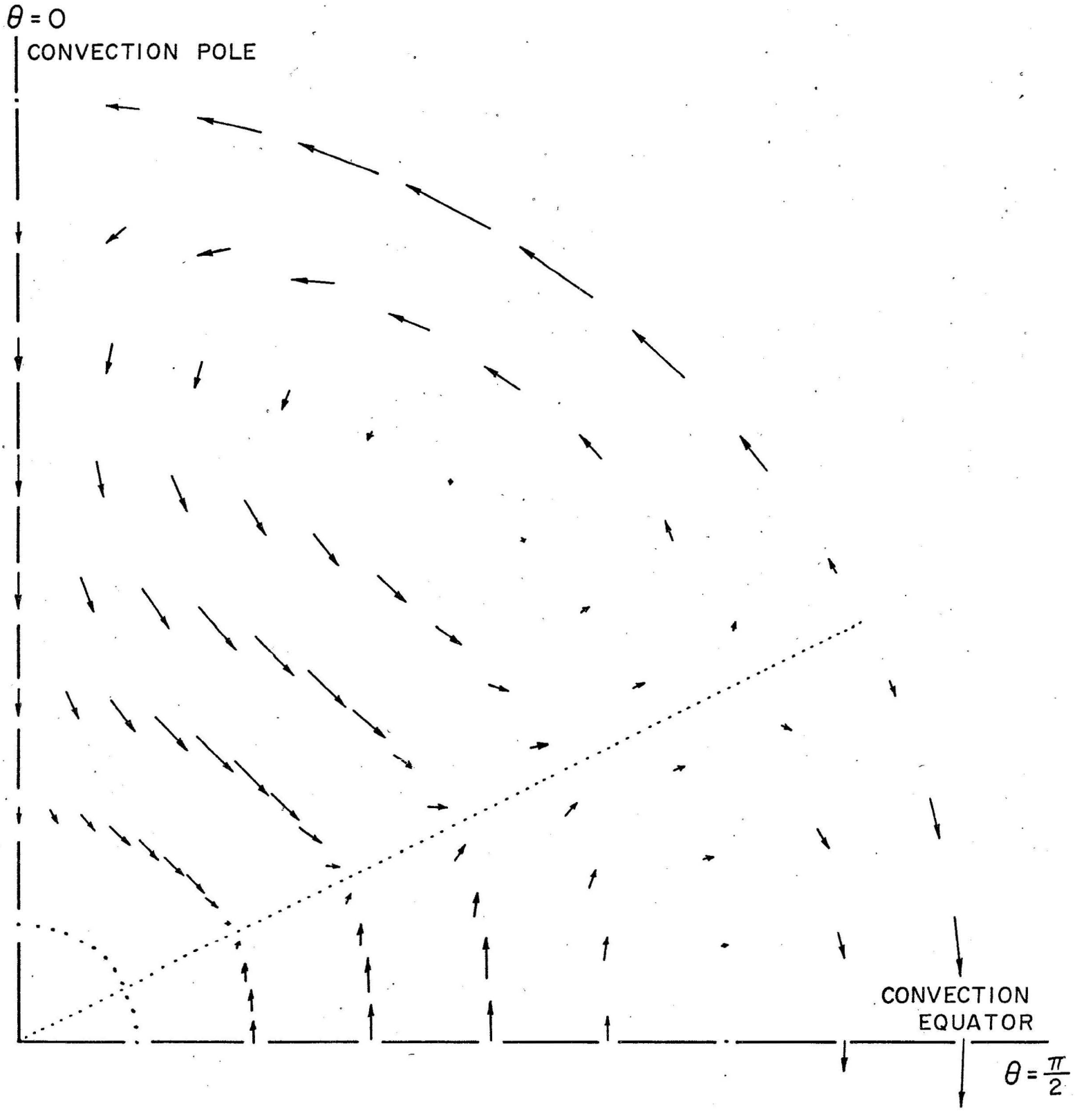

Figure 7. Relative magnitudes and directions of the fluid velocities in a cross-sectional plane from the incipient growth rate solution for $n = 3$ with an outer free boundary, $\sigma = 0$ and uniform viscosity ($\epsilon = 0$).

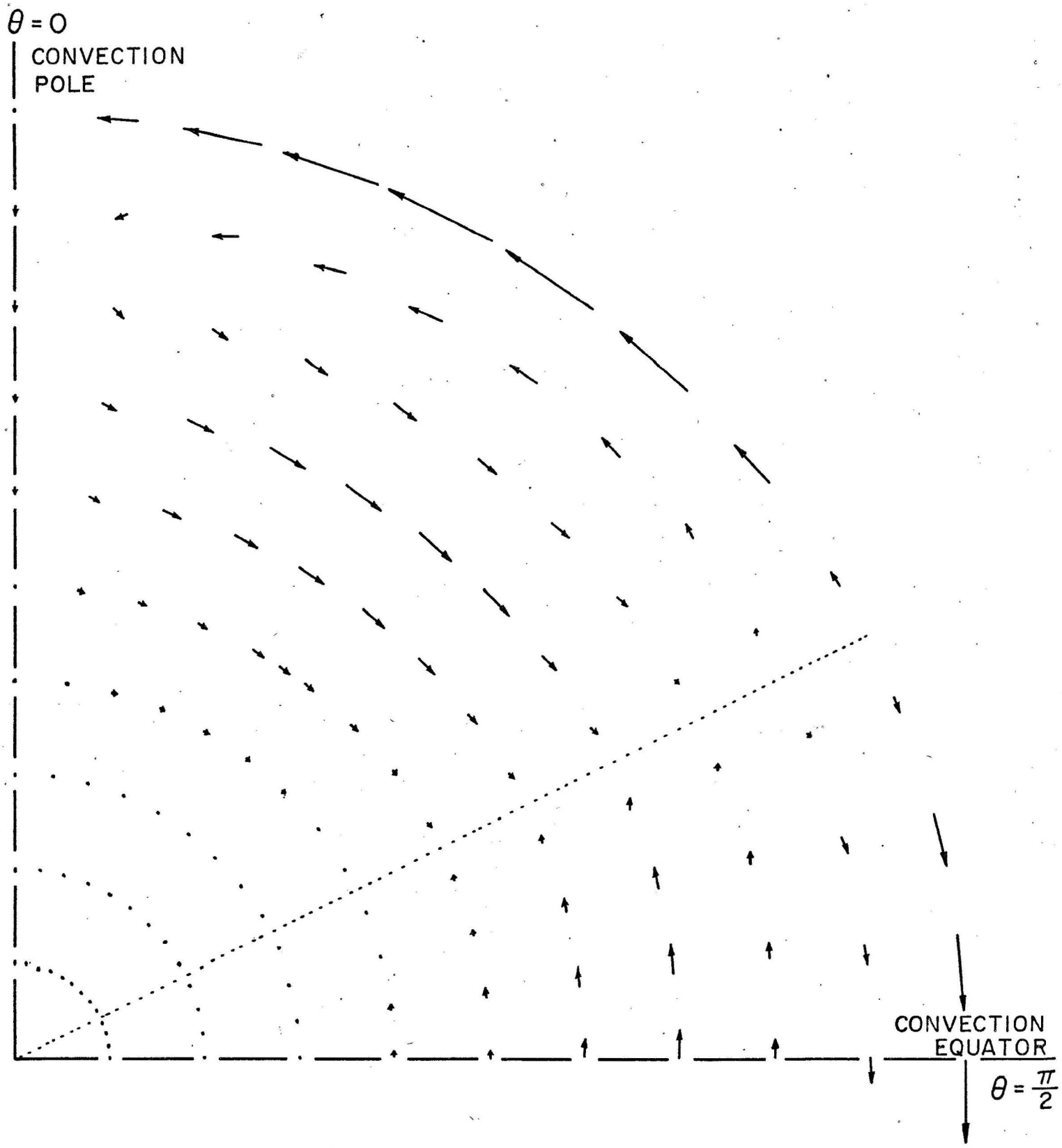

Figure 8. Relative magnitudes and directions of the fluid velocities in a cross-sectional plane from the incipient growth rate solution for $n = 3$ with an outer free boundary, $\sigma = 0$ and a viscosity which increases with depth according to $\epsilon = -5$.

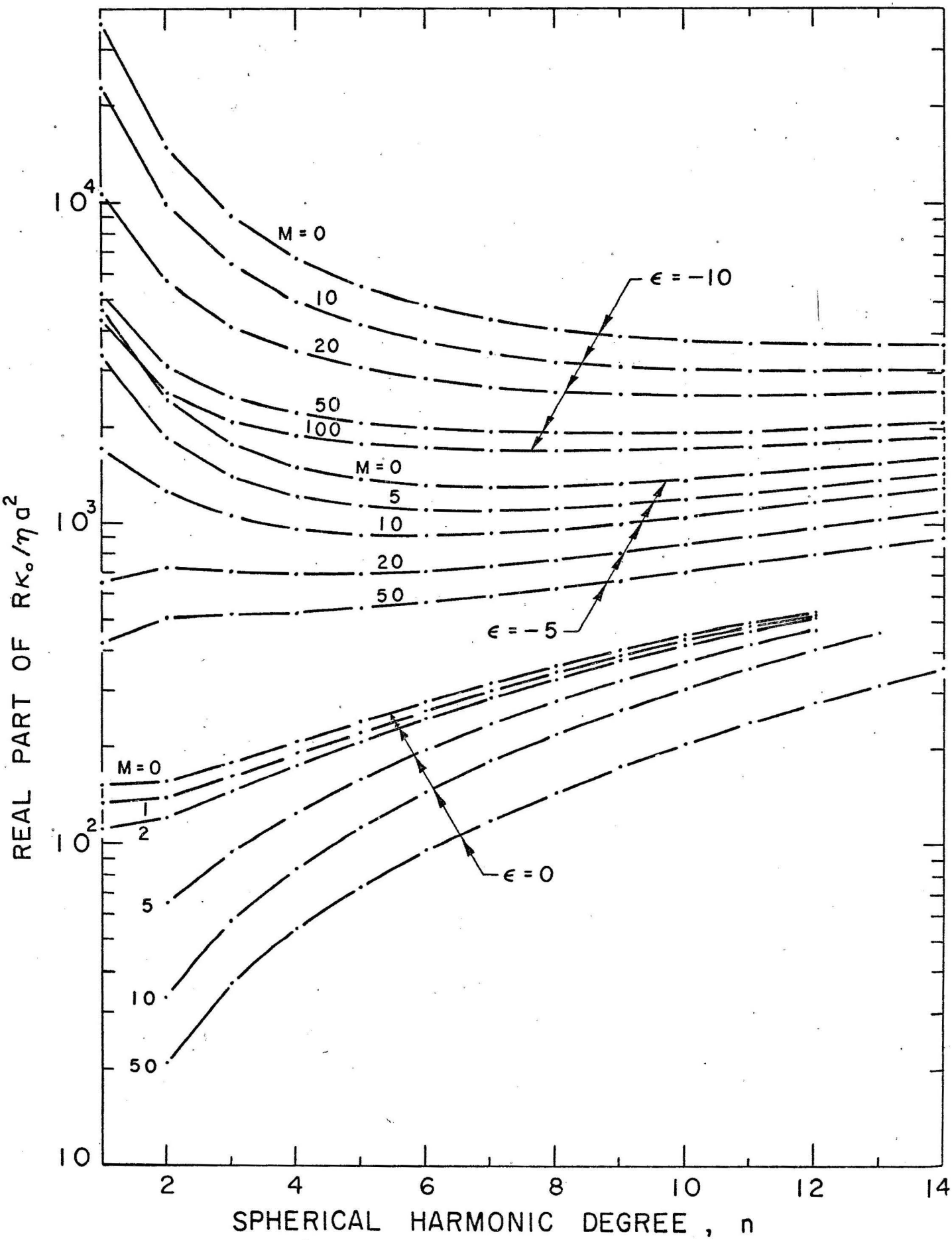

Figure 9. Results of the supercritical thermal convection growth rate calculation with a true free surface condition and various values of ϵ representing the increase of viscosity with depth and parameter $M = 2\beta\alpha a^2$.